

Identifying Disappearance of a White Dwarf Binary with LISA

Naoki Seto

Department of Physics, Kyoto University, Kyoto 606-8502, Japan

17 May 2023

ABSTRACT

We discuss the prospect of identifying a white dwarf binary merger by monitoring disappearance of its nearly monochromatic gravitational wave. For a ten-year operation of the laser interferometer space antenna (LISA), the chance probability of observing such an event is roughly estimated to be 20%. By simply using short-term coherent signal integrations, we might determine the merger time with an accuracy of ~ 3 -10 days. Also considering its expected sky localizability ~ 0.1 - 0.01deg^2 , LISA might make an interesting contribution to the multi-messenger study on a merger event.

Key words: gravitational waves — binaries: close

1 INTRODUCTION

LISA is expected to detect $\sim 10^4$ white dwarf binaries (WDBs) in our Galaxy as nearly monochromatic gravitational wave (GW) sources (Hils, Bender, & Webbink 1990; Nelemans et al. 2001; Nissanke et al. 2012; Breivik et al. 2018; Lamberts et al. 2019; Amaro-Seoane et al. 2022). Their GW frequencies slightly change due to the radiation reaction, and the majority of them are considered to merge eventually. Given the estimated Galactic merger rate $R \sim 0.02\text{yr}^{-1}$ (see e.g., Nelemans et al. 2001), we might actually have a merger event with a chance probability of $\sim 0.2(T/10\text{yr})$, during LISA’s operation period T .

A WDB merger in our Galaxy will be an intriguing observational target for multi-messenger astronomy (see e.g., Schwab 2018 and also Shen et al. 2012; Dan et al. 2014) and can help our understanding of white dwarfs (potentially including their explosion process). As an omni-directional GW detector free from interstellar extinction, LISA can provide us with critical information (e.g. sky locations, orbital phases) for follow-up electromagnetic (EM) searches (e.g., Korol et al. 2017). Therefore, in this paper, we discuss identification of a WDB merger in LISA’s data.

From various estimations (Amaro-Seoane et al. 2022 and references therein), the majority of merging WDBs are likely to have total masses less than $1M_{\odot}$. In the connection to type Ia supernovae, one might be interested in WDBs with the total masses larger than the Chandrasekhar mass. However, their merger rate is estimated to be $\sim 5 - 7$ times smaller than the total rate quoted above (Nelemans et al. 2001, see also Maoz, Hallakoun, & Badenes 2018).

According to recent numerical simulations with a care-

ful treatment for the initial conditions (Dan et al. 2011 see also Benz et al. 1990; Rasio & Shapiro 1992; D’Souza et al. 2006; Lorén-Aguilar, Isern, & García-Berro 2009; Raskin et al. 2012; Pakmor et al. 2013), a typical merging WDB will continue to emit nearly monochromatic GW, until just before the donor star is tidally disrupted and the system virtually turns off GW emission. On the basis of this overall GW emission pattern, we examine a forceful approach for the identification of a WDB merger by repeatedly checking the resultant disappearance of its nearly monochromatic GW. We pay an attention to the estimation of the merger time, which will be important for EM observations.

This paper is organized as follows. In §2, we briefly describe the evolution of a merging WDB and the associated GW emission. In §3, we discuss LISA’s observation for the GW signal, including estimation of the merger time with matched filtering analysis. In §4, we discuss related topics such as the cases with other space interferometers. §5 is devoted to a short summary.

2 EVOLUTION OF A MERGING WDB

2.1 Nearly Monochromatic Waves

As an approximation to a detached WDB emitting a nearly monochromatic GW, we briefly discuss a circular binary composed by two point masses m_1 and m_2 ($m_1 \leq m_2$). Using the Kepler’s law, we can write down the wave frequency

$$f = \pi^{-1} G^{1/2} (m_1 + m_2)^{1/2} a^{-3/2} \quad (1)$$

with the orbital separation a and the gravitational constant G . At the quadrupole order, the angular averaged strain

arXiv:2305.09061v1 [astro-ph.HE] 15 May 2023

amplitude is written as

$$h = \frac{8G^{5/3}\mathcal{M}^{5/3}\pi^{2/3}f^{2/3}}{5^{1/2}c^4d} \quad (2)$$

with the distance d to the binary (below fixed at the representative distance $d = 10\text{kpc}$) and the speed of light c (Robson, Cornish, & Liu 2019). Here we put the chirp mass $\mathcal{M} \equiv (m_1m_2)^{3/5}(m_1+m_2)^{-1/5}$.

The frequency evolution due to the radiation reaction is written as

$$\begin{aligned} \frac{df}{dt} &= \frac{96G^{5/3}\pi^{8/3}\mathcal{M}^{5/3}f^{11/3}}{5c^5} \quad (3) \\ &= 2.5 \times 10^{-6} \left(\frac{f}{20.8\text{mHz}}\right)^{11/3} \left(\frac{\mathcal{M}}{0.38M_\odot}\right)^{5/3} \text{Hz yr}^{-1}. \end{aligned}$$

The tidal interaction between the two star will modify our expressions (1)-(3) to some extent (e.g., $\sim 10\%$ for Eq. (3) as in Wolz et al. 2021). However, in this paper, we are mainly interested in the identification of a WDB merger event from LISA's data, by just using the disappearance of its GW (not trying to accurately estimate e.g., its chirp mass). Later, we use Eq. (2) in this context, and it will work reasonably well, up to very close to the final merger (Dan et al. 2011).

Given the merger rate (or more appropriately the merger flux) R of Galactic WDBs, we can apply the continuity equation in the frequency space and approximately evaluate their frequency distribution dN/df as

$$\begin{aligned} \frac{dN}{df} &\sim R(df/dt)^{-1} \quad (4) \\ &\sim 3.4 \times 10^6 \left(\frac{R}{0.02\text{yr}^{-1}}\right) \left(\frac{f}{4\text{mHz}}\right)^{-11/3} \text{Hz}^{-1}. \quad (5) \end{aligned}$$

This expression will be valid in the frequency regime $f \lesssim 10\text{mHz}$ where the merger flux R is expected to be nearly constant (Seto 2022). Here, for simplicity, we ignored the chirp mass distribution and put $\mathcal{M} = 0.38M_\odot$. From an integral of Eq. (5), the number of Galactic WDBs above $\sim 4\text{mHz}$ is roughly estimated to be $N(> 4\text{mHz}) \sim 5 \times 10^3$.

2.2 Transition around the Merger

Due to the radiation reaction, the orbital separation of a detached WDB decreases gradually and the less massive donor m_1 will eventually fill its Roche-lobe, initiating mass transfer to the accreter m_2 (Paczynski 1967; Marsh, Nelemans, & Steeghs 2004). The time evolution during this mass transfer phase has been examined by numerical simulations (Dan et al. 2011). A typical merging WDB (like those analyzed below) will continue to emit nearly monochromatic GW (roughly described in the previous subsection), until the donor loses a small fraction of its mass due to an unstable mass transfer (see e.g., Figs 7 and 17 in Dan et al. 2011).

Then, in a short transitional period Δt_t (corresponding to $\lesssim 10$ wave cycles), the donor is tidally disrupted, and the system will soon settle down into a nearly axisymmetric configuration, virtually stopping GW emission (Dan et al. 2011, see also Yoshida 2021; Moran-Fraile et al. 2023). We define the merger time t_m as the beginning of the transition period Δt_t . One of our primary objectives below is to clarify how well we can observationally determine the merger time t_m only with LISA.

Table 1. Nearly monochromatic GWs from merging WDBs (A: our base model, B: the lower mass model, C: the higher mass model). We put the donor mass m_1 and the accreter mass m_2 . The binary merges around the frequency f_m . We show the signal-to-noise ratios ρ during the final two years before the merger with LISA (at the distance of $d = 10\text{kpc}$). We present the short-term integration period T_s to get signal-to-noise ratio of $\rho_{\text{th}} = 7.5$. The corresponding rotation cycles $f_m \cdot T_s$ are also presented.

| model | A (base) | B | C |
|------------------------------------|---------------|---------------|---------------|
| m_1 | $0.4 M_\odot$ | $0.3 M_\odot$ | $0.6 M_\odot$ |
| m_2/m_1 | 1.2 | 1.2 | 1.5 |
| f_m | 20.8 mHz | 15.0 mHz | 35.1 mHz |
| ρ ($T = 2\text{yr}$) | 85 | 47 | 210 |
| T_s ($\rho_{\text{th}} = 7.5$) | 5.7 day | 18.6 day | 0.93 day |
| $f_m \cdot T_s$ | 10000 | 24000 | 2800 |

We also define the merger frequency f_m as the GW frequency at end of the nearly monochromatic emission (just before the transition period). Similarly, we put the associated characteristic strain amplitude h_m which is obtained by plugging in the final frequency $f = f_m$ in Eq. (2).

Next, following Marsh, Nelemans, & Steeghs (2004), let us approximately estimate the merger frequency f_m , by using the condition of the Roche-lobe filling of the less massive (donor) star m_1 . We apply the mass radius relation $r(m_1)$ for completely degenerate helium given in Verbunt & Rappaport (1988), ignoring (potentially existing) diffuse outer envelope. Meanwhile the Roche-lobe radius is approximately given by Paczyński (1967) as

$$R_L = 2 \cdot 3^{-4/3} m_1^{1/3} (m_1 + m_2)^{-1/3} a. \quad (6)$$

Then we put $R_L = r(m_1)$ for the donor m_1 at the onset of the mass overflow. From Eqs. (1) and (6), the merger frequency is written as

$$f_m(m_1) = \frac{2^{3/2}G^{1/2}m_1^{1/2}}{9\pi r(m_1)^{3/2}}, \quad (7)$$

depending only on the mass m_1 of the donor.

In this paper, considering the mass distribution of WDBs, we examine the three WDB models presented in Table 1. We set the model A as the base model for our study with the lower-mass comparative model B. The reference model C has the total mass of $1.5M_\odot$. In Table 1, we present their merger frequencies (7). From a comparison with a more detailed numerical study in Dan et al. (2011), our rough estimation is expected to have accuracy within $\sim 15\%$ for the presented donor masses m_1 .

At the frequency $f_m = 20.8\text{mHz}$, under the point particle approximation the base model A has the radiation reaction time scale $f/\dot{f} \sim 10^4\text{yr}$. Therefore, even $\sim 10\text{yr}$ before the merger, we approximately have its frequency and amplitude as $f \sim f_m$ and $h \sim h_m$.

2.3 Evolutionary Stages

On the basis of the previous two subsections, we next divide the time evolution of a merging WDB into the four stages (i)-(iv), as a preparation for the matched filtering analysis mainly discussed in the next section.

For coherent signal integration with the matched filter-

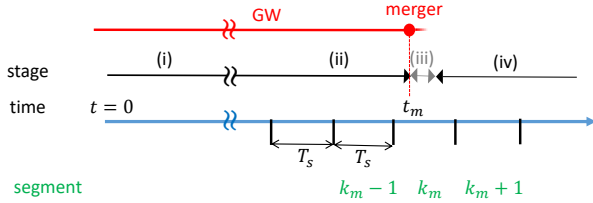


Figure 1. Schematic diagram for observation of a GW signal from a merging WDB. We set the time origin $t = 0$ at the beginning of LISA’s operation and put the merger time by $t = t_m$. We divide the time sequence into the four stages (i)-(iv) with the duration Δt_p and Δt_t respectively for (ii) and (iii). For the identification of the merger time t_m , we introduce the time segmentation with an appropriately selected duration T_s . The merger time t_m is in the segment $k = k_m$.

ing analysis, the phase of the target GW should be accurately characterized by a limited number of fitting parameters (e.g., the polynomial expansion with the derivative coefficients $f^{(n)}$ at some epoch). Unlike a well separated WDBs, even in the time region of nearly monochromatic GW emission, a WDB close to the merger might have complicated GW phase modulations which should be handled with a short-term phenomenological phase modeling. As a precaution for such a potential difficulty, we conservatively divide the time region of nearly monochromatic emission into two stages (i) and (ii). We put Δt_p as the total duration of the late monochromatic stage (ii). Sorting out the temporal sequence, around the merger time t_m , we now have the following four stages.

(i) Early monochromatic stage at $t < t_m - \Delta t_p$. The binary emits nearly monochromatic GW at the frequency $\sim f_m$ with the amplitude $\sim h_m$. Its intrinsic GW phase can be coherently described by a simple expression.

(ii) Late monochromatic stage at $t_m - \Delta t_p < t < t_m$. The binary continues to emit nearly monochromatic wave at $\sim f_m$ and $\sim h_m$. We need phenomenological phase model with a short integration period.

(iii) Transition stage at $t_m < t < t_m + \Delta t_t$. The disruption of the donor proceeds rapidly and the emitted GW no longer has regular monochromatic pattern, due to hydrodynamical effects.

(iv) Post-merger stage at $t_m + \Delta t_t < t$. Virtually no GW is emitted, as the merged system settles down to a nearly stationary and axisymmetric configuration.

Here we can practically assume $\Delta t_p \gg \Delta t_t$ (otherwise we do not need to introduce the late stage (ii)). In contrast to the transition duration Δt_t deduced from existing numerical simulations, the magnitude of Δt_p is currently unclear. We need to accurately follow the longer-term dynamical evolution at high mass resolution. Numerical approach would be highly demanding, and analytical study might be more advantageous. Observational studies on known short-period WDBs might be also useful (see e.g. Strohmayer 2021; Mun-

day et al. 2023 for RX J0806.3+1527). Below, we leave the duration Δt_p as a free parameter, just assuming $\Delta t_p \ll 1\text{yr}$. We should also comment that the boundary between (i) and (ii) is not mathematically distinct. It is rather a practical one and depends on the complexity of the phase modeling allowed for the stage (i).

3 OBSERVATION WITH LISA

Next we discuss matched filtering analysis with LISA. We set the origin of the time coordinate $t = 0$ at the beginning of LISA’s operation. Given its planned operation period 4-10 yr, we below set $t_m = 2\text{yr}$ as a conservative average. For the purpose of concise illustration, we are assumed to make two kinds of data analysis: the long-term search and the segmented short-term search.

The purpose of the long-term search is to confidently detect a WDB and determine its basic parameters, using the data at the early monochromatic stage (i). This search would be similar to the signal analysis for a standard (non-merging) WDB. Using the results of the long-term search, we subsequently perform the segmented short-term searches for identifying the disappearance of its nearly monochromatic GW at the merger. In reality, we can chronologically mix these two searches.

3.1 The Long-Term Search

Throughout the early monochromatic stage (i), the GW signal would be coherently searched with manageable numerical costs. The total signal-to-noise ratio ρ can be estimate as

$$\rho = \frac{h_m \sqrt{T}}{S_n(f_m)^{1/2}} \quad (8)$$

for the integration time T . Here, for simplicity, we ignore the angular dependence of the GW strain (Cutler 1998). It is straightforward to include it in our analysis below.

As presented in Table 1 for $T = t_m = 2\text{yr}$, the expected signal-to-noise ratio in the stage (i) is $\rho = O(100)$ and much larger than those for typical Galactic LISA sources existing at lower frequencies. For the base model A (up to the end of the stage (ii)), the signal-to-noise ratio squared ρ^2 increases unity in every ~ 180 wave cycles, corresponding to ~ 0.1 day (~ 430 cycles for B and ~ 50 cycles for C). Therefore, even though the catastrophic stage (iii) is interesting, this stage is likely to have a negligible contribution to the signal-to-noise ratio, given its rotation cycles of $\lesssim 10$ (Dan et al. 2011). For our signal analysis scheme, we can omit the stage (iii) and effectively regard that the nearly monochromatic stage (ii) is directly followed by the quiet stage (iv) at the merger time t_m .

Using the high quality signal in the stage (i), we can securely confirm the existence of the binary. We can also estimate its nearly monochromatic frequency f_m and other basic parameters including the amplitude h_m . For instance, the sky position of the binary can be determined with the aid of the Doppler modulation (Cutler 1998). For $T \gtrsim 2\text{yr}$, we can apply an asymptotic scaling relation for the area of

the error ellipsoid (Takahashi & Seto 2002)

$$\Delta\Omega \sim 0.01 \left(\frac{\rho}{85}\right)^{-2} \left(\frac{f}{20.8\text{mHz}}\right)^{-2} \text{deg}^2. \quad (9)$$

The area becomes $\sim 0.06\text{deg}^2$ for the model B. The high sky localization would be beneficial for associated EM observations.

3.2 Segmented Short-Term Search

Let us suppose that we have already done the long-term search for a WDB, in the middle of its early monochromatic stage (i). Now, we divide the upcoming data streams into segments of a duration T_s as shown in Fig. 1. We assign the label k and put ρ_k for the corresponding signal-to-noise ratio obtained after the short-term coherent matched filtering. The total number of the segments increases, as LISA's operation period becomes longer.

Our immediate goal is to observationally determine the specific segment k_m which contains the merger time t_m (see Fig. 1). To this end, we appropriately set the threshold ρ_{th} and the duration T_s , so that we can reliably have $\rho_k \geq \rho_{\text{th}}$ for earlier segments $k < k_m$ and $\rho_k < \rho_{\text{th}}$ for later segments $k > k_m$, due to the existence of the nearly monochromatic wave before the merger time t_m .

Here, in terms of statistical tests, we want to suppress the false dismissal rate P_{FDR} for $k < k_m$ and the false alarm rate P_{FAR} for $k > k_m$, both caused by the flukes of the noise realizations (Buonanno, Chen, & Vallisneri 2003). We should notice that, for the target WDB, presupposing the high-quality information from the already analyzed data (in the stage (i)), the implication of these two rates are somewhat different from the blind short-lived binary search with the current LVK network (The LIGO Scientific Collaboration et al. 2021).

For a segment at $k > k_m$, assuming Gaussian noise, the false alarm rate is estimated to be

$$P_{\text{FAR}} = \frac{\mathcal{N}}{\sqrt{2\pi}} \int_{\rho_{\text{th}}}^{\infty} \exp\left[-\frac{\rho^2}{2}\right] d\rho = \frac{\mathcal{N}}{2} \text{erfc}\left[\frac{\rho_{\text{th}}}{2^{1/2}}\right] \quad (10)$$

with the effective number of the templates \mathcal{N} and the complementary error function $\text{erfc}(\cdot)$. Note that the function $\text{erfc}\left[\frac{\rho_{\text{th}}}{2^{1/2}}\right]/2$ depends very strongly on ρ_{th} and we have $10^{-2}, 10^{-3}, 10^{-5}$ and 10^{-7} respectively for $\rho_{\text{th}} = 2.3, 3.1, 4.3$ and 5.2 . The effective number of templates \mathcal{N} depends on the possible phase models (and the integration time T_s). After all, in our pilot study, we shifted the uncertainty of the stage (ii) to that of the template number \mathcal{N} . In the actual data analysis, we can use the information of the earlier segments, for empirically extending the phase models. At present, on the basis of the strong dependence on ρ_{th} , we adopt the reference value $\rho_{\text{th}} = 5$ for $P_{\text{FAR}} = 10^{-2}$. If we actually have $\Delta t_p \ll T_s$, our setting $\rho_{\text{th}} = 5$ will result in a very conservative choice.

Next we discuss the false dismissal rate for an earlier segment $k < k_m$. Using the results (e.g., h_m and f_m) from the preceding long-term search, we can estimate the expectation value

$$\langle\rho_k\rangle = \frac{h_m\sqrt{T_s}}{S_n(f_m)^{1/2}} \quad (11)$$

as a function of the segment duration T_s . Then, by adjusting the duration T_s , we can evaluate the false dismissal rate as

$$P_{\text{FDR}} = \frac{1}{\sqrt{2\pi}} \int_{-\infty}^{\rho_{\text{th}}} \exp\left[-\frac{(\rho - \langle\rho_k\rangle)^2}{2}\right] d\rho \quad (12)$$

$$= \frac{1}{2} \text{erfc}\left[\frac{\langle\rho_k\rangle - \rho_{\text{th}}}{2^{1/2}}\right]. \quad (13)$$

For $P_{\text{FDR}} \sim 10^{-2}$, we have

$$\langle\rho_k\rangle \simeq \rho_{\text{th}} + 2.5 = 7.5. \quad (14)$$

We can inversely obtain the segment duration T_s by

$$T_s = \langle\rho_k\rangle^2 S_n(f_m) h_m^{-2}. \quad (15)$$

In Table 1, we present the numerical results for T_s , together with the corresponding rotation cycles $f_m \cdot T_s$. For the base model, we have $T_s = 5.7$ day and 10000 cycles.

From the arguments so far, we can easily see that, for the critical segment $k = k_m$, we have $\rho_k \geq \rho_{\text{th}}$ or $\rho_k < \rho_{\text{th}}$, depending on the location of the merger time t_m in the segment.

3.3 Estimation of the Merger Time

Next we discuss the estimation of the merger time t_m from the growing list $\{\rho_k\}$ obtained after repeating the short-term matched filtering. To proceed in a dualistic manner, we map the signal-to-noise ratios ρ_k by

$$F_k \equiv \theta(\rho_k - \rho_{\text{th}}) \quad (16)$$

with the step function $\theta(\cdot)$. We will have $F_k = 1$ for $k < k_m$ and $F_k = 0$ for $k > k_m$ ($F_k = 1$ or 0 for $k = k_m$). Then, the list $\{F_k\}$ should have the following form

$$\{F_k\} = \{1, 1, \dots, 1, \underline{1}, 0, 0, 0, \dots\}. \quad (17)$$

The merger time t_m should be contained in the two specific segments marked with the underline. Therefore, the half width δt_m of the estimation error becomes

$$\delta t_m = 2^{-1}(2T_s) = T_s. \quad (18)$$

So far, we have fixed the segmentation. By relaxing this setting, we can further analyze the two candidate segments above. More specifically, we put a slidable segment characterized by the starting time x (keeping the duration at T_s) as

$$k(x) \equiv [x, x + T_s]. \quad (19)$$

We define the associated signal-to-noise ratio $\rho(x)$ for this segment. We can identify the maximum value $x = x_{\text{max}}$ which satisfies $F[\rho(x)] = 1$. Similarly, we read the minimum value $x = x_{\text{min}}$ for $F[\rho(x)] = 0$ with $x_{\text{max}} \leq x_{\text{min}}$. Here, the inequality can be caused by an intricate pattern of the function $F[\rho(x)]$ due to the noise. The merger time t_m should be contained simultaneously in the two segments $k(x_{\text{max}})$ and $k(x_{\text{min}})$. Taking their overlapped part, we can estimate the merger time with a half width of

$$\delta t_m \leq T_s/2, \quad (20)$$

corresponding to $\lesssim 3$ days for our base model.

The estimated magnitude δt_m is much larger than the transition period Δt_t around the merger. Therefore, as mentioned earlier, we practically do not need to too rigidly define

the merger time t_m (e.g., before or after the transition stage (iii)).

4 DISCUSSION

So far, we have discussed matched filtering analysis for a merging Galactic WDB with LISA. Here, from a broader perspective, we mention related topics and potential extension of this work.

4.1 GW data analysis

We have assumed $\Delta t_p \ll 1\text{yr}$, for the duration Δt_p of the late monochromatic stage (ii). Currently, it is not straightforward to solidly estimate the duration Δt_p introduced for precautionary purpose. As already commented, we can rather evaluate the potential phase evolution, by empirically using the existing earlier data of the binary (smoothly from the stage (i)). Similarly, the number of effective templates \mathcal{N} will be estimated reasonably well at the actual data analysis in the stage (ii).

In a very pessimistic scenario with $\Delta t_p \gtrsim 2\text{yr}$, we might not have the simple stage (i), which has played a key role in our data analysis procedure. A semi-coherent search could be a powerful option, as currently applied to unknown pulsar search with the LVK network (Abbott et al. 2022). GW from a WDB could be observed at much higher signal-to-noise ratio with much smaller rotation cycles. Therefore, depending on the phase irregularity, our task could be much easier than the unknown pulsar search with the LVK network.

At estimating the merger time t_m , we have used a matched filtering analysis just for checking the disappearance of a nearly monochromatic GW signal (without decoding its detailed structure). In reality, the wave phase might be relatively simple with a precursor signature for the forthcoming merger. Then, we might predict the merger time t_m by carefully performing matched filtering analysis. If this is the case, our estimation δt_m should be regarded as a very conservative bound. On another front, while we have introduced the mapping (16) for our simple dualistic argument, the original function $\rho(x)$ can be directly analyzed for the estimation of the merger time t_m .

Note that, if the operation period of LISA is longer than $\sim 1\text{yr}$, the Galactic confusion noise is negligible in the frequency regime $f \gtrsim 5\text{mHz}$ (Robson, Cornish, & Liu 2019; Littenberg et al. 2020). Therefore, for a donor mass $m_1 \gtrsim 0.3M_\odot$ shown in Table 1, the interference with other binary signals is likely to be insignificant. However, we have $f_m \sim 5\text{mHz}$, for a smaller donor mass $m_2 \sim 0.1M_\odot$. For such a binary, we might need to securely suppress the interference effects at the LISA multi source-analysis. Consequently, the required segment duration T_s could be longer than that estimated from Eq. (11).

We can try other efficient methods (e.g., the chi-square analysis), particularly in the context of the low latency analysis. The non-Gaussianity of detector noises might be also worth studying.

4.2 Other Space Interferometers

Here we briefly comment on space interferometers other than LISA. Since a WDB mainly emits a nearly monochromatic GW, our results scale simply with the instrumental noise spectrum $S_n(f)$, as shown in Eqs. (8) and (15).

Around 20mHz, the sensitivities of Taiji (Ruan et al. 2018) and TianQin (Luo et al. 2016) are quite similar and approximately two times better than that of LISA. Meanwhile, at $\sim 20\text{mHz}$, B-DECIGO (Kawamura et al. 2021) is designed to have a sensitivity similar to LISA, but its optimal band is in the higher frequency regime around 100mHz (Isoyama, Nakano, & Nakamura 2018). B-DECIGO and its follow-on mission DECIGO (Seto, Kawamura, & Nakamura 2001) might thereby enable us to detect extra-Galactic merging WDBs with total masses higher than the Chandrasekhar mass (possibly relevant for SNIa) (Maselli, Marassi, & Branchesi 2020; Kinugawa et al. 2022).

4.3 EM Observation

When we try to identify an EM counterpart to a WDB, its binary parameters (e.g., those related to orbital phase, sky location and inclination) will be critically useful. Once identified, we can continue to frequently observe the binary with EM telescopes, even after the operation period of LISA. Moreover, we might monitor the transitional merger stage (iii) with the telescopes. Such an observation will provide us with valuable information on white dwarfs and, possibly, its explosion mechanism. The archived data much before LISA's launch might be also useful for studying a WDB in a long time span (Digman & Hirata 2022).

5 SUMMARY

The merger rate of Galactic WDBs is roughly estimated to be $\sim 0.02\text{yr}^{-1}$. In this paper, we discuss identification of a merger event in the data streams of LISA. Until very close its final merger, a typical WDB will emit nearly monochromatic GW around 20mHz. After a short transition period, it will virtually stop emitting GW. LISA has potential to detect its nearly monochromatic GW with a signal-to-noise ratio of $O(10^2)$ and determine its sky location within $\sim 0.01\text{-}0.1\text{deg}^2$. By repeatedly checking the disappearance of its nearly monochromatic GW, we could robustly estimate its merger time with accuracy of $\sim 3\text{-}10$ days.

ACKNOWLEDGEMENTS

This work is supported by JSPS Kakenhi Grant-in-Aid for Scientific Research (Nos. 17H06358, 19K03870 and 23K03385).

REFERENCES

Abbott R., Abe H., Acernese F., Ackley K., Adhikari N., Adhikari R. X., Adkins V. K., et al., 2022, *PhRvD*, 106, 102008. doi:10.1103/PhysRevD.106.102008

- Amaro-Seoane P., Andrews J., Arca Sedda M., Askar A., Balasov R., Bartos I., Bavera S. S., et al., 2022, arXiv, arXiv:2203.06016. doi:10.48550/arXiv.2203.06016
- Benz W., Bowers R. L., Cameron A. G. W., Press W. H., 1990, ApJ, 348, 647. doi:10.1086/168273
- Breivik K., Kremer K., Bueno M., Larson S. L., Coughlin S., Kalogera V., 2018, ApJL, 854, L1. doi:10.3847/2041-8213/aaaa23
- Buonanno A., Chen Y., Vallisneri M., 2003, PhRvD, 67, 024016. doi:10.1103/PhysRevD.67.024016
- Cutler C., 1998, PhRvD, 57, 7089. doi:10.1103/PhysRevD.57.7089
- Dan M., Rosswog S., Guillochon J., Ramirez-Ruiz E., 2011, ApJ, 737, 89. doi:10.1088/0004-637X/737/2/89
- Dan M., Rosswog S., Brügggen M., Podsiadlowski P., 2014, MNRAS, 438, 14. doi:10.1093/mnras/stt1766
- Digman M. C., Hirata C. M., 2022, arXiv, arXiv:2212.14887. doi:10.48550/arXiv.2212.14887
- D'Souza M. C. R., Motl P. M., Tohline J. E., Frank J., 2006, ApJ, 643, 381. doi:10.1086/500384
- Hils D., Bender P. L., Webbink R. F., 1990, ApJ, 360, 75. doi:10.1086/169098
- Isoyama S., Nakano H., Nakamura T., 2018, PTEP, 2018, 073E01. doi:10.1093/ptep/pty078
- Kawamura S., Ando M., Seto N., Sato S., Musha M., Kawano I., Yokoyama J., et al., 2021, PTEP, 2021, 05A105. doi:10.1093/ptep/ptab019
- Kinugawa T., Takeda H., Tanikawa A., Yamaguchi H., 2022, ApJ, 938, 52. doi:10.3847/1538-4357/ac9135
- Korol V., Rossi E. M., Groot P. J., Nelemans G., Toonen S., Brown A. G. A., 2017, MNRAS, 470, 1894. doi:10.1093/mnras/stx1285
- Lamberts A., Blunt S., Littenberg T. B., Garrison-Kimmel S., Kupfer T., Sanderson R. E., 2019, MNRAS, 490, 5888. doi:10.1093/mnras/stz2834
- Littenberg T. B., Cornish N. J., Lackeos K., Robson T., 2020, PhRvD, 101, 123021. doi:10.1103/PhysRevD.101.123021
- Lorén-Aguilar P., Isern J., García-Berro E., 2009, A&A, 500, 1193. doi:10.1051/0004-6361/200811060
- Luo J., Chen L.-S., Duan H.-Z., Gong Y.-G., Hu S., Ji J., Liu Q., et al., 2016, CQGra, 33, 035010. doi:10.1088/0264-9381/33/3/035010
- Maoz D., Hallakoun N., Badenes C., 2018, MNRAS, 476, 2584. doi:10.1093/mnras/sty339
- Marsh T. R., Nelemans G., Steeghs D., 2004, MNRAS, 350, 113. doi:10.1111/j.1365-2966.2004.07564.x
- Maselli A., Marassi S., Branchesi M., 2020, A&A, 635, A120. doi:10.1051/0004-6361/201936848
- Moran-Fraile J., Schneider F. R. N., Roepke F. K., Ohlmann S. T., Pakmor R., Soutanis T., Bauswein A., 2023, arXiv, arXiv:2303.05519
- Munday J., Marsh T. R., Hollands M., Pelisoli I., Steeghs D., Hakala P., Breedt E., et al., 2023, MNRAS, 518, 5123. doi:10.1093/mnras/stac3385
- Nelemans G., Yungelson L. R., Portegies Zwart S. F., Verbunt F., 2001, A&A, 365, 491. doi:10.1051/0004-6361:20000147
- Nissanke S., Vallisneri M., Nelemans G., Prince T. A., 2012, ApJ, 758, 131. doi:10.1088/0004-637X/758/2/131
- Paczyński B., 1967, AcA, 17, 287
- Pakmor R., Kromer M., Taubenberger S., Springel V., 2013, ApJL, 770, L8. doi:10.1088/2041-8205/770/1/L8
- Rasio F. A., Shapiro S. L., 1992, ApJ, 401, 226. doi:10.1086/172055
- Raskin C., Scannapieco E., Fryer C., Rockefeller G., Timmes F. X., 2012, ApJ, 746, 62. doi:10.1088/0004-637X/746/1/62
- Robson T., Cornish N. J., Liu C., 2019, CQGra, 36, 105011. doi:10.1088/1361-6382/ab1101
- Ruan W.-H., Guo Z.-K., Cai R.-G., Zhang Y.-Z., 2018, arXiv, arXiv:1807.09495. doi:10.48550/arXiv.1807.09495
- Ruiter A. J., Belczynski K., Benacquista M., Larson S. L., Williams G., 2010, ApJ, 717, 1006. doi:10.1088/0004-637X/717/2/1006
- Schwab J., 2018, MNRAS, 476, 5303. doi:10.1093/mnras/sty586
- Seto N., Kawamura S., Nakamura T., 2001, PhRvL, 87, 221103. doi:10.1103/PhysRevLett.87.221103
- Seto N., 2022, PhRvL, 128, 041101. doi:10.1103/PhysRevLett.128.041101
- Shen K. J., Bildsten L., Kasen D., Quataert E., 2012, ApJ, 748, 35. doi:10.1088/0004-637X/748/1/35
- Strohmayer T. E., 2021, ApJL, 912, L8. doi:10.3847/2041-8213/abf3cc
- Takahashi R., Seto N., 2002, ApJ, 575, 1030. doi:10.1086/341483
- The LIGO Scientific Collaboration, the Virgo Collaboration, the KAGRA Collaboration, Abbott R., Abbott T. D., Acernese F., Ackley K., et al., 2021, arXiv, arXiv:2111.03606. doi:10.48550/arXiv.2111.03606
- Verbunt F., Rappaport S., 1988, ApJ, 332, 193. doi:10.1086/166645
- Wolz A., Yagi K., Anderson N., Taylor A. J., 2021, MNRAS, 500, L52. doi:10.1093/mnras/slaa183
- Yoshida S., 2021, ApJ, 906, 29. doi:10.3847/1538-4357/abc7bd